

Supporting Information for
Constructing Active Copper Species in Cu-Zeolite for
Coal-gas-SCR and Elucidating Synergistic Catalytic Function of
CuO and Cu²⁺ Ion Species

Jie Cheng, Dahai, Zheng, Chengna Dai, Ruinian Xu*, Ning Liu, Gangqiang Yu, Ning
Wang, and Biaohua Chen

Faculty of Environment and Life, Beijing University of Technology, Beijing 100124,
China

*Corresponding Authors: Ruinian Xu

xuruinian@bjut.edu.cn (R. Xu)

Content	3
S1. Catalysts preparation	3
S2. Catalysts characterization.....	3
S3. Catalyst activity test	5
S4. Computational methods and constructed models	6
S5. Ab initio thermodynamic analysis.....	7
S6. SCR activity	9
S7. Physicochemical property characterization.....	14
S8. H ₂ -TPR results.....	16
S9. EPR results	17
S10. XPS results	18
S11. DFT calculations	19
S12. <i>In situ</i> DRIFTS studies.....	30
References	34

Content

S1. Catalysts preparation

A commercial H-ZSM-5 ($\text{SiO}_2/\text{Al}_2\text{O}_3=25$) zeolite support was purchased from Nankai University Catalyst Co., Ltd. Cu-ZSM-5 catalysts in present work were prepared by using a liquid ion exchange and co-precipitation method reported by our group.¹ In a typical synthesis procedure, a certain amount of $\text{Cu}(\text{NO}_3)_3 \cdot 3\text{H}_2\text{O}$ was dissolved in 200 ml deionized water, then 5 g calcined H-ZSM-5 zeolite power were added into the above solution under continuously stirring at 80 °C. After 24 h stirring, the slurry was filtered and thoroughly washed with deionized water. Subsequently, the resulting solid was dried at 100 °C for 12 h. In order to increase more exchanged copper species, the procedure was repeated two times and the Cu loading was detected by ICP-AES. The obtained samples denoted as Cu-ZSM-5-IE.

As for Cu-ZSM-5-IE+CP, after the ion-exchange, the samples were calcined at 550 °C for 6 h. Afterward, the power was added into the solution containing required amount of $\text{Cu}(\text{NO}_3)_3 \cdot 3\text{H}_2\text{O}$ which were calculated to keep the total Cu loading is 3%, then the 0.5 M NaOH solution was dropped under vigorously stirred until the pH value reached approximately 9. After being stirred for 3 h, the sediments were finally washed with deionized water three times. Then the solid was dried at 100 °C for 12 h and calcined at 550 °C for 6 h in air with a ramp rate of 10 °C min^{-1} . As for Cu-ZSM-5-CP catalyst, the procedures is similar to the previous preparation process, except that the ion exchange process is omitted, and also keep the total Cu loading is 3%.

The commercial H-ZSM-5 ($\text{SiO}_2/\text{Al}_2\text{O}_3=25$), H-Y ($\text{SiO}_2/\text{Al}_2\text{O}_3=5.1$), H-SSZ-13 ($\text{SiO}_2/\text{Al}_2\text{O}_3=20$), H-SAPO-34 ($\text{SiO}_2/\text{Al}_2\text{O}_3=0.5$), and H-SUZ-4 ($\text{SiO}_2/\text{Al}_2\text{O}_3=5.1$) zeolite support were purchased from Nankai University Catalyst Co., Ltd. The Cu-ZSM-5 catalyst was synthesized by wetness impregnation method. In this procedure, NH_4 -ZSM-5 zeolite was calcined at 550 °C in air for 6 h to remove some residual NH_4^+ and leave it for later use. 1 g $\text{Cu}(\text{NO}_3)_3 \cdot 3\text{H}_2\text{O}$ was dissolved in 400 ml deionized water, then 5 g calcined H-ZSM-5 zeolite power was added into the above solution under continuously stirring at 80 °C for 4 h, the slurry was then placed in 90 °C bath and rotated to evaporate the excess water. Subsequently, the resulting solid was dried at 100 °C for 12 h and calcined at 550 °C for 6 h in air with a ramp rate of 10 °C min^{-1} . The obtained samples denoted as Cu-ZSM-5. And the Cu-SUZ-4, Cu-SSZ-13, Cu-SAPO-34, and Cu-Y catalyst were also prepared using this method.

S2. Catalysts characterization

The XRD signals were recorded in 2θ range of 5-70 ° with a step size of 0.02 °. The zeolite phases were determined by comparing the obtained results with IZA reference.

H₂-TPR experiments was carried out in a fixed-bed reactor with 100 mg samples and pretreated with 30 mL min⁻¹ He flow at 500 °C for 2 h. After cooling down to 100 °C, the sample was exposed to 30 mL min⁻¹ of 5% H₂/Ar and heated from 100 to 900 °C at a rate of 5 °C min⁻¹ to guarantee the all copper species could be completely reduced. The signal of hydrogen consumption was collected by a TCD detector, and the H₂ consumption of all the samples were calculated using CuO as the corresponding standard sample.

The EPR spectrometer equipped with a Bruker EMX PLUS resonator and a continuous flow cryostat. The samples (~20 mg) were putted in quartz tubes and sealed with a rubber septa. Spectra were recorded at 150 K temperature and the field was swept from 2000 to 5000 G with 2.5 G amplitude. In addition, microwave power used for tests was 200 microwatts, and the frequency of that was 9.86 GHz.

UV-vis diffuse-reflectance spectra were conducted in the range of 200-800 nm over Shimadzu UV-3600Plus spectrometer under the ambient condition, wherein the samples of Cu-ZSM-5 samples were ground into BaSO₄. Prior to testing, the three samples were treated at 500 °C for 1 h in a flow of 30 mL min⁻¹ He atmosphere, subsequently exposed to the gas mixture of 250 ppm NO + 450 ppm CO + 2400 ppm H₂ + 1200 ppm CH₄+ 6% O₂ for 1 h at 300 °C, then the samples were tested and compared with the fresh sample.

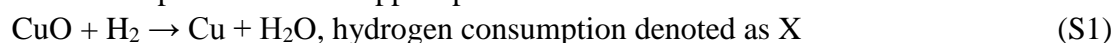
NO + O₂-TPD experiments were performed on mass spectrometer (QMS 403 QUADRO) instrument to detect the desorption amount of NO. Before the NO adsorption, the catalyst was treated at 500 °C for 1 h in a flow of 30 mL min⁻¹ He atmosphere. After cooling down to 50 °C, the catalyst were exposed to 250 ppm NO + 6% O₂ for 1 h and then purged with He. Subsequently, the catalyst was heated in He flow from 50-700 °C at a rate of 10 °C min⁻¹ and the signal of NO was detected by mass spectrometer.

For evidencing the direct transfer of intermediates, SCR-TPD experiments were conducted. Firstly, the CuO was treated at 500 °C for 1 h and then exposed to 250 ppm NO + 6% O₂ at 150 °C for 1 h. The Cu-ZSM-5-IE was also treated at 500 °C for 1 h and then exposed to 450 ppm CO + 2400 ppm H₂ + 1200 ppm CH₄+ 6% O₂ at 150 °C for 1 h. For in tight contact configuration, the as-saturated 50 mg NO_x adsorbed CuO and 100 mg reductants adsorbed Cu-ZSM-5-IE were grinded in mortar to ensure uniform mixing and tight contact, named as CuO/Cu-ZSM-5-IE. For dual-layer configuration, 100 mg reductants adsorbed Cu-ZSM-5-IE was placed downstream of 50 mg NO_x adsorbed CuO, and two catalysts was separated by a thin layer of quartz wool in the middle, named as CuO+Cu-ZSM-5-IE. Subsequently, the two configurations were exposed to He atmosphere in the flow of 30 mL min⁻¹, then the signals of products were monitored by MS with the temperature increasing from 100-700 °C at a rate of 10 °C min⁻¹.

The copper surface area and dispersion of the catalyst were analyzed on AutoChem II 2920 apparatus using N₂O chemisorption and H₂ pulse reduction method. Firstly, the samples were treated at 850 °C in the flow of 5% H₂/Ar for 4 h, the first H₂ consumption was detected by TCD detector and denoted as X, then cooled down to 60 °C. Subsequently, pure N₂O was introduced into the sample cell for 1 h to completely oxidize copper atoms into Cu₂O species, then H₂ pulse reduction were performed at 400 °C to guarantee all the chemisorbed oxygen could be thoroughly

reacted with H₂ and the second H₂ consumption was denoted as Y. The copper surface area and dispersion were calculated based on the equation reported by Van Der Grift et al.^{2,3}

The first step reduction of copper species:



The second step reduction of copper species:



The dispersion (D) and surface area (S) of copper were calculated as

$$D = (2 \times Y/X) \times 100\% \quad (\text{S3})$$

$$S = 2 \times Y \times N_{\text{av}} / (X \times M_{\text{Cu}} \times 1.4 \times 10^{19}) \quad (\text{S4})$$

$$= 1353 \times Y/X \text{ (m}^2\text{-Cu/g-Cu)} \quad (\text{S5})$$

Wherein, N_{av} is Avogadro's constant, M_{Cu} is the relative atomic mass of copper (63.46 g/mol), and the 1.4 × 10¹⁹ is the number of copper atom of per square meter.

The temperature programmed surface reaction (TPSR) experiment was conducted over a fixed-bed reactor system being connected with a mass spectrometer (QMS 403 QUADRO). Initially, the catalyst sample of 100 mg was pretreated by He) for 1 h at 500 °C; then the gas mixture of 250 ppm NO + 450 ppm CO + 2400 ppm H₂ + 1200 ppm CH₄+ 6% O₂ balanced by He and with a total flow rate of 129 mL min⁻¹ was introduced into the reactor being heated at a rate of 5 °C min⁻¹; simultaneously, the M/e signals were recorded by the mass spectrometer with multiple ion detection (MID), which includes 2 (H₂), 16 (CH₄), 18 (H₂O), 28 (CO/N₂), 30 (NO), 42 (NCO), 44 (CO₂/N₂O), 45 (CH₃NO), 46 (NO₂) and 61 (CH₃NO₂).

In situ DRIFTS experiments were conducted on FTIR spectrometer (Bruker Tensor II) with BaF₂ windows, which is equipped with liquid nitrogen cooled high-sensitive MCT detector. Prior to each experiment, the samples were pretreated at 500 °C for 1 h in a flow of 30 mL min⁻¹ He and then cooled to 100 °C. Afterwards, the background spectrum was recorded in the flow of He and was subtracted from the sample spectrum. Whereafter, the samples was exposed to a 30 ml min⁻¹ of 250 ppm NO + 6% O₂ at 280 °C for 1 h and then purged with He to remove NO from the gas phase and physical adsorption. Then the mixture of 450 ppm CO + 2400 ppm H₂ + 1200 ppm CH₄ were introduced to react with adsorbed NO in a flow of 50 mL min⁻¹. Subsequently, the spectra were recorded at 280 °C with different reaction time. Moreover, after reacting for 60 min, cut off the reducing agent and pass in NO + O₂ to continue the reaction while collecting spectra. All spectra were recorded from 4000 to 400 cm⁻¹ by accumulating 32 scans with a resolution of 4 cm⁻¹.

S3. Catalyst activity test

The SCR activity measurement was performed in a quartz fixed-bed reactor (0.6 cm i.d.) loading with 0.250 g catalyst under an atmosphere of 250 ppm NO, 1200 ppm CH₄, 2400 ppm H₂, 450 ppm CO and 6 vol% O₂, balanced by He with a total flow rate of 129 mL min⁻¹ corresponding to GHSV approximate 28,000 h⁻¹. The proportion of these reductants is settled according to the components of coke oven gas. Prior to activity test, the samples were treated at 500 °C for 2 h under He atmosphere. The

reactor was regulated continuously using a temperature controller with a thermocouple inserted into the catalyst bed achieving temperatures from 100 to 500 °C by steps of 50 °C. The effluent gases (CH₄, CO, N₂O, NO, and NO₂) were monitored using an infrared gas analyzer (Shimadzu IRTracer-100) equipped with a 2.4 meter long-path gas cell and IR solution analysis software. The outlet concentration of H₂ was monitored by a gas chromatograph (GC-4000A) with a TCD detector. The NO_x, CH₄, and CO conversions as well as N₂, N₂O, and NO₂ yields were calculated based on the following formulas:

$$NO_x \text{ conversion } (\%) = \frac{(NO)_{inlet} - (NO + NO_2 + 2N_2O)_{outlet}}{(NO)_{inlet}} \times 100 \quad (S6)$$

$$CO \text{ conversion } (\%) = \frac{(CO)_{inlet} - (CO)_{outlet}}{(CO)_{inlet}} \times 100$$

(S 7)

$$CH_4 \text{ conversion } (\%) = \frac{(CH_4)_{inlet} - (CH_4)_{outlet}}{(CH_4)_{inlet}} \times 100$$

(S 8)

$$H_2 \text{ conversion } (\%) = \frac{(H_2)_{inlet} - (H_2)_{outlet}}{(H_2)_{inlet}} \times 100$$

(S 9)

$$N_2 \text{ selectivity } (\%) = \frac{(2N_2)_{outlet}}{2(N_2)_{outlet} + 2(N_2O)_{outlet} + (NO_2)_{outlet}} \times 100$$

(S 10)

$$N_2O \text{ yield } (\%) = \frac{2(N_2O)_{outlet}}{(NO)_{inlet}} \times 100 \quad (S11)$$

$$NO_2 \text{ yield } (\%) = \frac{(NO_2)_{outlet}}{(NO)_{inlet}} \times 10 \quad (S12)$$

S4. Computational methods and constructed models

Periodic density functional theory (DFT) calculations were performed using the Vienna ab initio simulation package (VASP).⁴ The projector augmented wave (PAW) method combined with a plane wave basis set was used to describe the core and valence electrons.⁵ The exchange correlation effects are investigated within the generalized gradient approximation according to Perdew, Burke, and Ernzerhof (PBE).⁶ The spin-polarized calculations were also taken into account and the cutoff energy was set to 400 eV. All structures were relaxed until the forces over each atom were smaller than 0.05 eV Å⁻¹ and a Monkhorst-Pack k point of 2 × 2 × 1 was selected for the Brillouin zone integration. The MFI structure consists of 96 T atoms (T = Si, Al) and 192 oxygen atoms. The lattice parameters of MFI unit cell were set to

$a = 20.078 \text{ \AA}$, $b = 19.894 \text{ \AA}$, and $c = 13.372 \text{ \AA}$, which were retrieved from the IZA database.⁷ Among the 96 T sites, there are 12 different geometrically distinguishable T site that can be occupied by Al atom, and the geometrically optimized energy of different T sites were calculated to determine the most thermal stability structure and the construction of our model structure are displayed in Fig. S8-10. From the calculation results, the one Al in 10 members ring was chosen to locate in T12 site since it possessed the lowest energy.

CuO (111) surface structure was constructed by using a (2×2) supercell and a vacuum thickness of the model was set to 15 \AA to prevent other periodic cell from influencing the reaction. Moreover, the two layers at the bottom were frozen, whereas the top two layers used for the adsorption was relaxed.

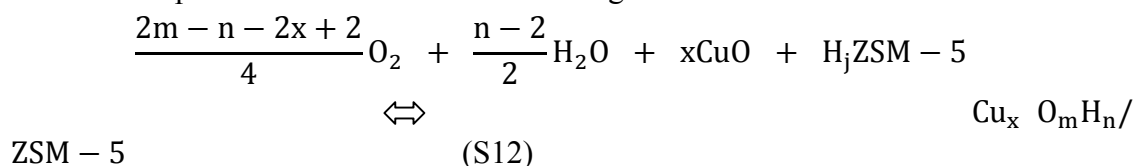
The Cu-ZSM-5 and CuO (111) model and adsorbed molecule were also optimized geometrically by VASP, and the adsorbed energy of those molecules are calculated following the formula:

$$\Delta E = E_{system} - E_{model} - E_{adsorbed}$$

Wherein, E_{system} represents the calculated electronic energy of the given geometry containing the zeolite and the adsorbed molecules, E_{model} is the calculated energy for Cu-ZSM-5 or CuO (111) model, and $E_{adsorbed}$ is the electronic energy for the adsorbed molecule attached to the Cu-ZSM-5 or CuO (111) model like CO, NO, CH₄ and so on. The adsorbed energy of those reactants on Cu-ZSM-5 or CuO (111) model are listed on Table S9-10.

S5. Ab initio thermodynamic analysis

Ab initio thermodynamics analysis was carried out to explore the influence of temperature and the chemical potential of H₂O and O₂ on the relative stability of the Cu complexes in Cu/ZSM-5. Bulk CuO and the H-form of ZSM-5 zeolite were used as the reference states in this analysis. The formation free energies (ΔG_{form}) are calculated according to the **Sq. 14-16** and used HSE06-TSvdw energies, the $\Delta\mu_O$ and $\Delta\mu_{H_2O}$ are a function of T and P and the standard chemical potentials of ideal gas as a reference. The relationship between diverse active centers structure with different chemical compositions were described following the reversible reactions:



wherein the x, m, and n respectively represent the atomic numbers of Cu, O, and H of the copper structure; and j represents the number of occupied Brönsted acid site in each active center structure;

The reaction Gibbs free energy ΔG were calculated following the equilibrium Eq. S13:

$$\Delta G(T, p) = G_{Cu_x O_m H_n / ZSM-5}^S - G_{H_j ZSM-5}^S - xG_{CuO}^S$$

$$-\frac{2m-n-2x+j}{2}\mu_O^g - \frac{n-j}{2}\mu_{H_2O}^g \quad (S13)$$

In this formula, the $\mu_{H_2O}^g$ and μ_O^g of gas phase H₂O and O depend on T and P , which can be obtained based on Eq. S14-15 on the basis of the assumption of that the chemical potentials of O and H₂O at 0 K are equal to the related electronic energies.

$$\mu_O(T, p) = \frac{1}{2}E_{O_2} + \Delta\mu_O(T, p) \quad (S14)$$

$$\mu_{H_2O}(T, p) = E_{H_2O} + \Delta\mu_{H_2O}(T, p)$$

$$\Delta\mu_O(T, p) = \Delta\mu_O(T, p) + \frac{1}{2}RT \ln\left(\frac{p_{O_2}}{p_{O_2}^0}\right) = \frac{1}{2}\left[\Delta\mu_{O_2}(T, p) + RT \ln\left(\frac{p_{O_2}}{p_{O_2}^0}\right)\right] \quad (S15)$$

$$= \frac{1}{2}\left[H(T, p^0, O_2) - H(0K, p^0, O_2) - T(S(T, p^0, O_2) - S(0K, p^0, O_2)) + RT \ln\left(\frac{p_{O_2}}{p_{O_2}^0}\right)\right] \quad (S16)$$

The $\Delta\mu(T, p)$ and $\Delta\mu_{H_2O}(T, p)$ can be respectively calculated based on the enthalpy and entropy of standard state at $T = 0$ K and $p_0 = 1$ bar and can be derived from NIST-JANAF Thermochemical Tables.⁸

$$\Delta G(T, p) = \Delta E - \frac{2m-n-2x+j}{2}\Delta\mu_O - \frac{n-j}{2}\Delta\mu_{H_2O} \quad (S17)$$

$$\Delta E = E_{Cu_xO_mH_n} - E_{H_jZSM-5} - xE_{CuO} - \frac{2m-n-2x+j}{4}E_{O_2} - \frac{n-j}{2}E_{H_2O} \quad (S18)$$

As for Eq. S13, the contributions of vibration and PV to solids are largely neglected, thus the Gibbs free energies of Cu_xO_mH_n/ZSM-5, H_jZSM-5, CuO can be respectively approximated to be their electronic energies computed by DFT calculation.

In order to study the stability of Z[Cu(II)]-6R-D4h structure with different ligand in various synthesis and treatment conditions, we calculated the formation energies of Z[Cu(II)]-6R-D4h structure containing O and H related to O₂ and H₂O reference, and the calculation are follow those formulas:

$$\Delta G_{x,y}^{form}(T, \Delta\mu_{O_2}, \Delta\mu_{H_2O}) = \Delta E_{x,y}^{form} - T\Delta S_{x,y}^{form}(T) - \frac{x}{2}\left(\Delta\mu_{H_2O} - \frac{1}{2}\Delta\mu_{O_2}\right) - \frac{y}{2}\Delta\mu_{O_2} \quad (S19)$$

$$\Delta E_{x,y}^{form} = E_{Z_*CuH_xO_y} - E_{Z_*Cu} - \frac{x}{2}\left(E_{H_2O} - \frac{1}{2}E_{O_2}\right) - \frac{y}{2}E_{O_2} \quad (S20)$$

ΔS^{ST} is the difference in entropy between a free and adsorbate-covered site. According to literature,⁹ it is found that there is a significant difference between the harmonic oscillator approximation and actual entropies. Compared to dynamic simulations, a simple heuristic was proposed in which the difference is approximated

from the Sackur-Tetrode expression:

$$\Delta S_{x,y}^{ST} = (S_{Z_*CuH_xO_y} - S_{Z_*Cu}) \approx \frac{2}{3} k_B \ln \left[\left(\frac{2\pi M_{x,y} k_B T}{h^2} \right)^{3/2} \frac{V e^{5/2}}{N_A} \right] \quad (S21)$$

Wherein, $M_{x,y}$ represents the total mass of the adsorbed species and V is the supercell volume of the structure. This model roughly treats adsorbed species as retaining 2/3 of their gas-phase translational entropy, similar to that discovered for adsorbates at surfaces.

S6. SCR activity

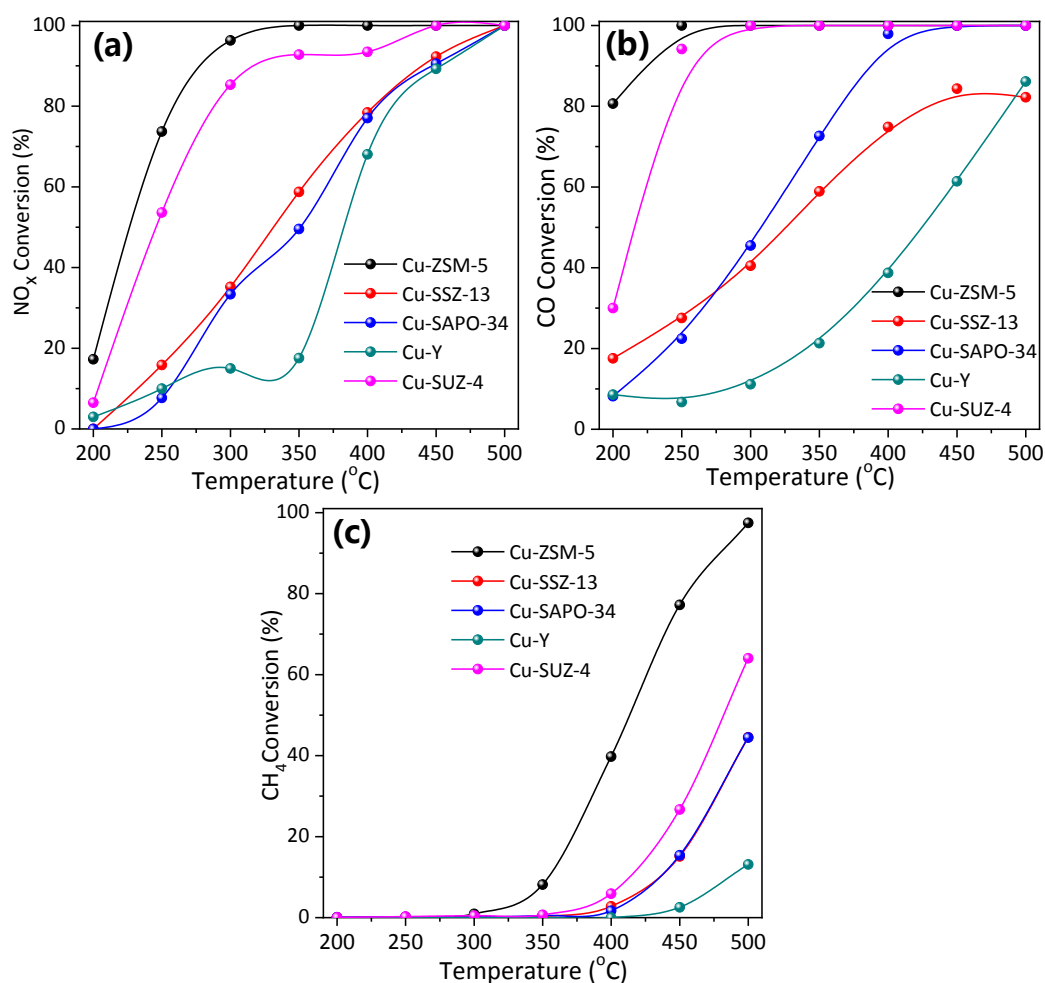


Fig. S1. (a) NO_x conversion, (b) CO conversion, and (c) CH₄ conversion of different samples with different topological structures. Reaction condition: 250 ppm NO, 1200 ppm CH₄, 2400 ppm H₂, 450 ppm CO, and 6 vol% O₂, balanced by He, and GHSV= 28,000 h⁻¹.

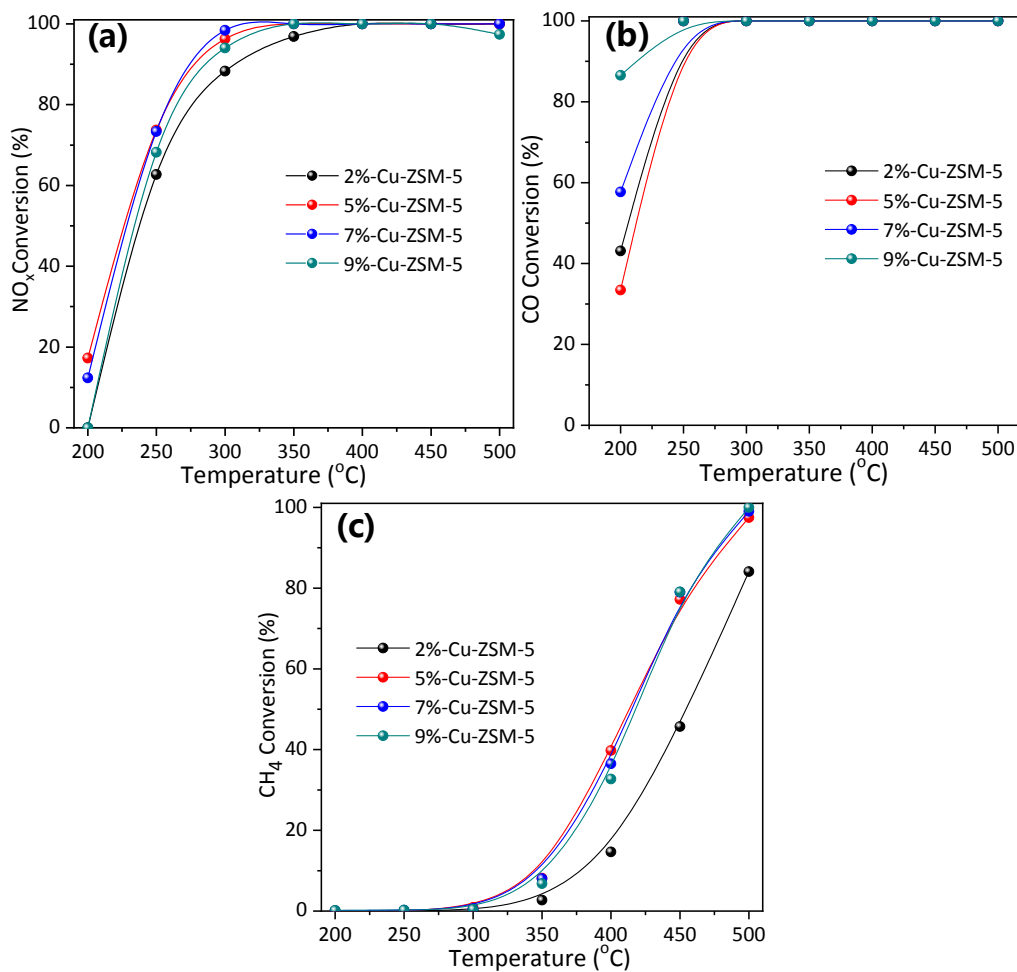


Fig. S2. (a) NO_x conversion, (b) CO conversion, and (c) CH₄ conversion of Cu-ZSM-5 with different Cu loading. Reaction condition: 250 ppm NO, 1200 ppm CH₄, 2400 ppm H₂, 450 ppm CO and 6 vol% O₂, balanced by He, and GHSV= 28,000 h⁻¹.

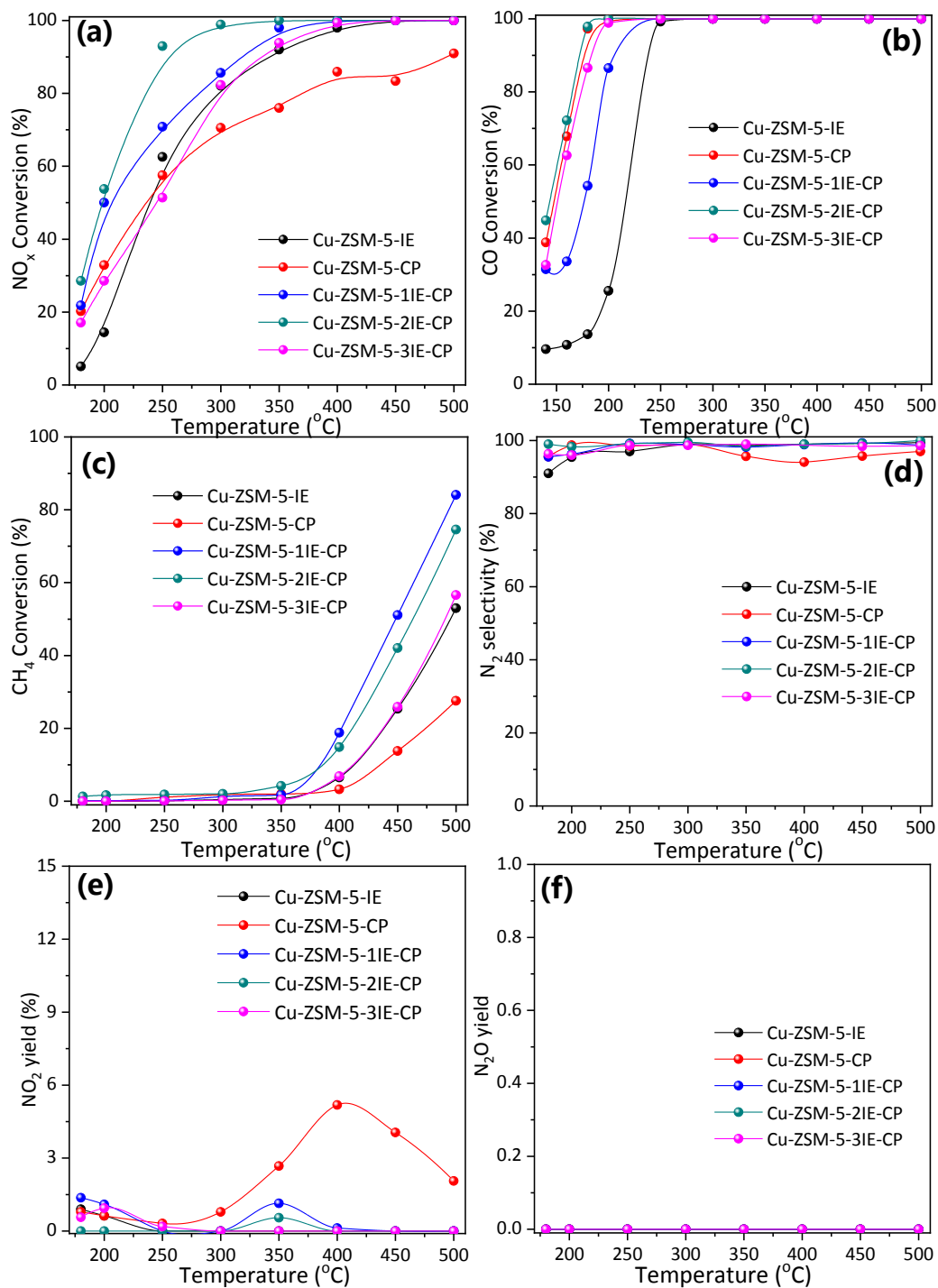


Fig. S3. (a) NO_x conversion, (b) CO conversion, (c) CH₄ conversion, (d) N₂ selectivity, (e) NO₂ yield, and (f) N₂O yield of Cu-ZSM-5 samples with different methods. Reaction condition: 250 ppm NO, 1200 ppm CH₄, 2400 ppm H₂, 450 ppm CO, 5% H₂O, and 6 vol% O₂, balanced by He, and GHSV= 28,000 h⁻¹.

Table S1. Quantities of elements in the investigated catalysts as measured by ICP.

Sample	Cu-ZSM-5- IE	Cu-ZSM-5- CP	Cu-ZSM-5- 1IE+CP	Cu-ZSM-5- 2IE+CP	Cu-ZSM-5- 3IE+CP
Si/Al ratio	15.60	16.70	16.30	16.31	16.12
Cu/Al ratio ^a	0.29	-	0.35	0.45	0.50
Cu ions loading (wt.%) ^b	1.90	-	2.12	2.81	3.13
Total Cu loading (wt.%) ^c	1.90	5.00	5.00	5.00	5.00
S _{BET} (m ² g ⁻¹)	301	252	270	283	285
Dispersion (%)	35.29	29.05	25.09	23.27	21.59
Metallic surface area (m ² g ⁻¹)	242.13	196.54	169.77	157.48	146.06
TOF (s ⁻¹) at 140 (°C) ^d	0.23	0.33	0.86	1.05	0.41

^a The Cu/Al ratio was calculated on the basis of the Cu ions loading (wt.%)

^b The Cu ions loading was the value of Cu that loaded by ion exchange manner.

^c The total Cu loading was determined by Cu ions + Cu in CuO.

^d TOF: the turnover frequency, the moles of NO reduced per mole of Cu per second.

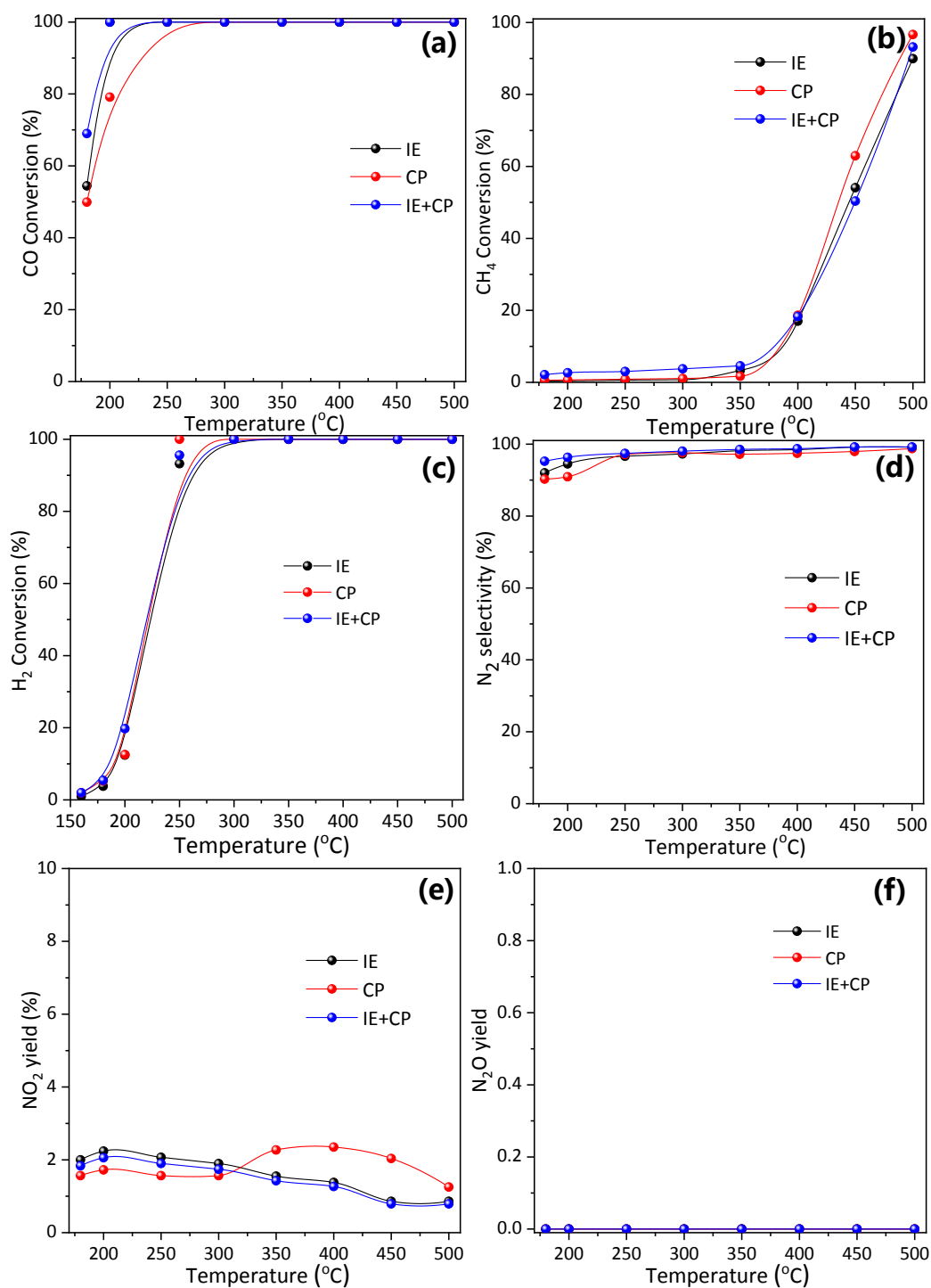


Fig. S4. (a) CO conversion, (b) CH₄ conversion, (c) H₂ conversion, (d) N₂ selectivity, (e) NO₂ yield, and (f) N₂O yield of 3% Cu-ZSM-5 samples with different methods. Reaction condition: 250 ppm NO, 1200 ppm CH₄, 2400 ppm H₂, 450 ppm CO, 5% H₂O, and 6 vol% O₂, balanced by He, and GHSV = 28,000 h⁻¹.

S7. Physicochemical property characterization

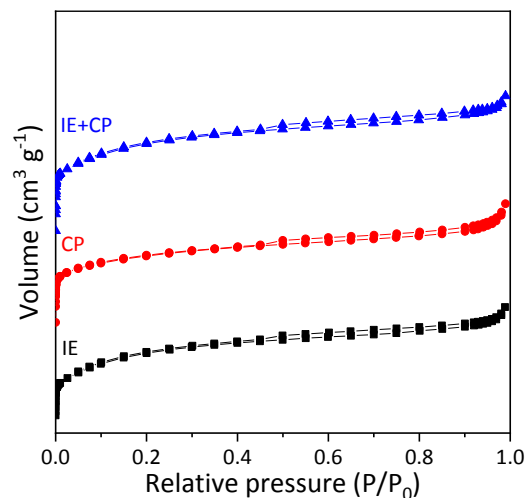


Fig. S5. Isothermal adsorption curves based on N₂ adsorption/desorption of 3% Cu-ZSM-5 samples.

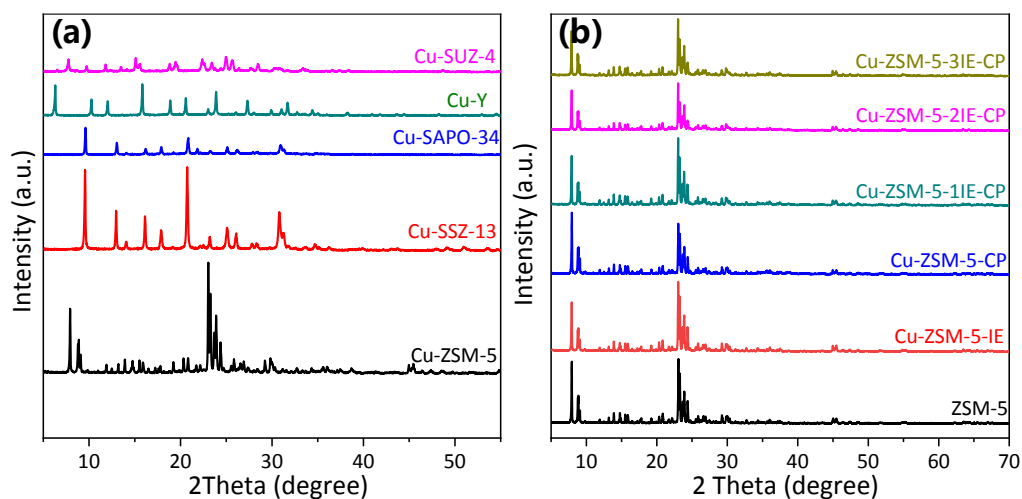


Fig. S6. XRD patterns of Cu-zeolite samples with different topological structures.

As shown in Fig. S6, those 5 kinds of zeolite catalysts have apparent diffraction peak of topological structure, which indicated that the introduction of Cu ions did not destroy the zeolite structure. Moreover, the characteristic diffraction peak of CuO ($2\theta=35.5$ and 38.8°) were not obviously detected in all catalysts, which may be caused by the high dispersion of CuO species or less amount than the XRD detect limit.

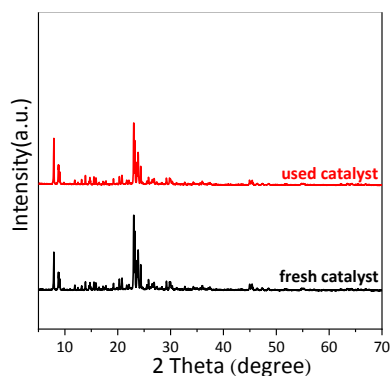


Fig. S7. XRD patterns of the fresh and used Cu-ZSM-5-IE+CP catalysts.

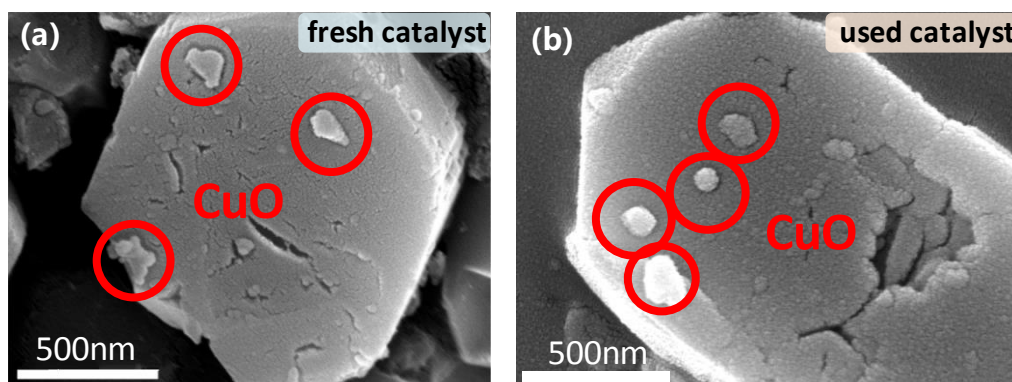


Fig. S8. HAADF-SEM images of the (a) fresh and (b) used Cu-ZSM-5-IE+CP catalysts.

Table S2. The BET surface area, pore volume, and pore size of the fresh and used Cu-ZSM-5-IE+CP catalysts.

Sample	S_{BET} ($\text{m}^2 \text{g}^{-1}$)	Pore Volume ($\text{cm}^3 \text{g}^{-1}$)
fresh sample	386.23	0.16
used sample	361.32	0.15

Note that, in **Fig. S7**, there is no characteristic diffraction peak of CuO ($2\theta = 35.5$ and 38.8°) appearing in the fresh and used catalysts, indicating that no aggregation of Cu species occurred during the reaction process. Besides, from SEM spectra of fresh and spent catalysts in **Fig. S8**, it can be also found that no obvious aggregated CuO particles formed on the surface of the used catalyst compared to the fresh sample. From SEM and XRD results, it can conclude that Cu-ZSM-5-IE+CP is sufficient stability in coal-gas-SCR reaction process.

S8. H₂-TPR results

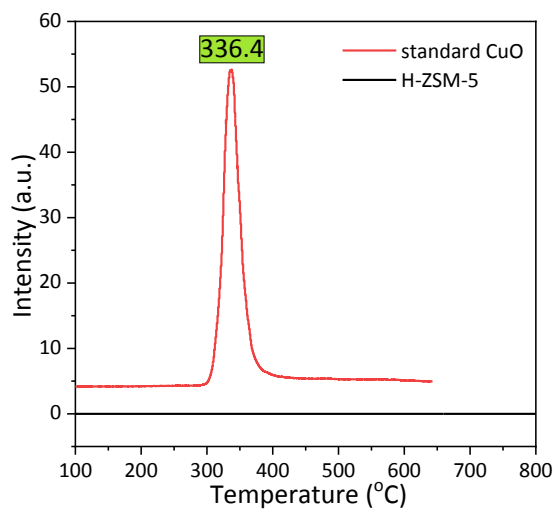


Fig. S9. The H₂-TPR curves of standard CuO and H-ZSM-5 samples.

Fig. S9 shows the H₂-TPR spectra of standard CuO and H-ZSM-5 samples. From the spectra, we can obviously know that H-ZSM-5 samples did not have apparent reduction peak in the temperature of 100-800 °C, while, standard CuO species only have a strong reduction signal at 336.4 °C, and the H₂ consumption of other samples were calculated on the basis of the H₂-TPR signal of standard CuO species.

S9. EPR results

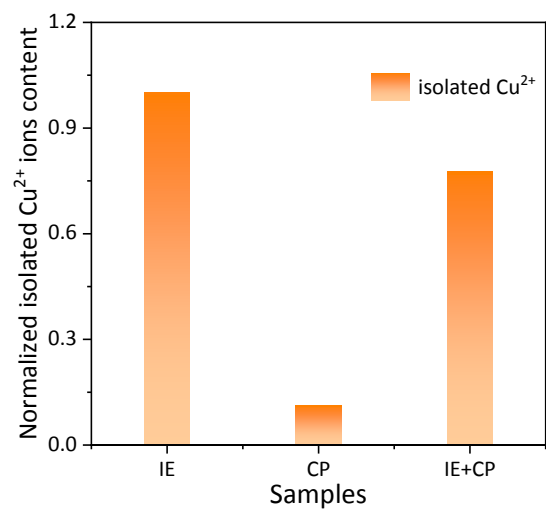


Fig. S10. The relative concentration of isolated Cu²⁺ species semiquantified by the EPR spectra over Cu-ZSM-5-IE, Cu-ZSM-5-CP, and Cu-ZSM-5-IE+CP catalysts.

S10. XPS results

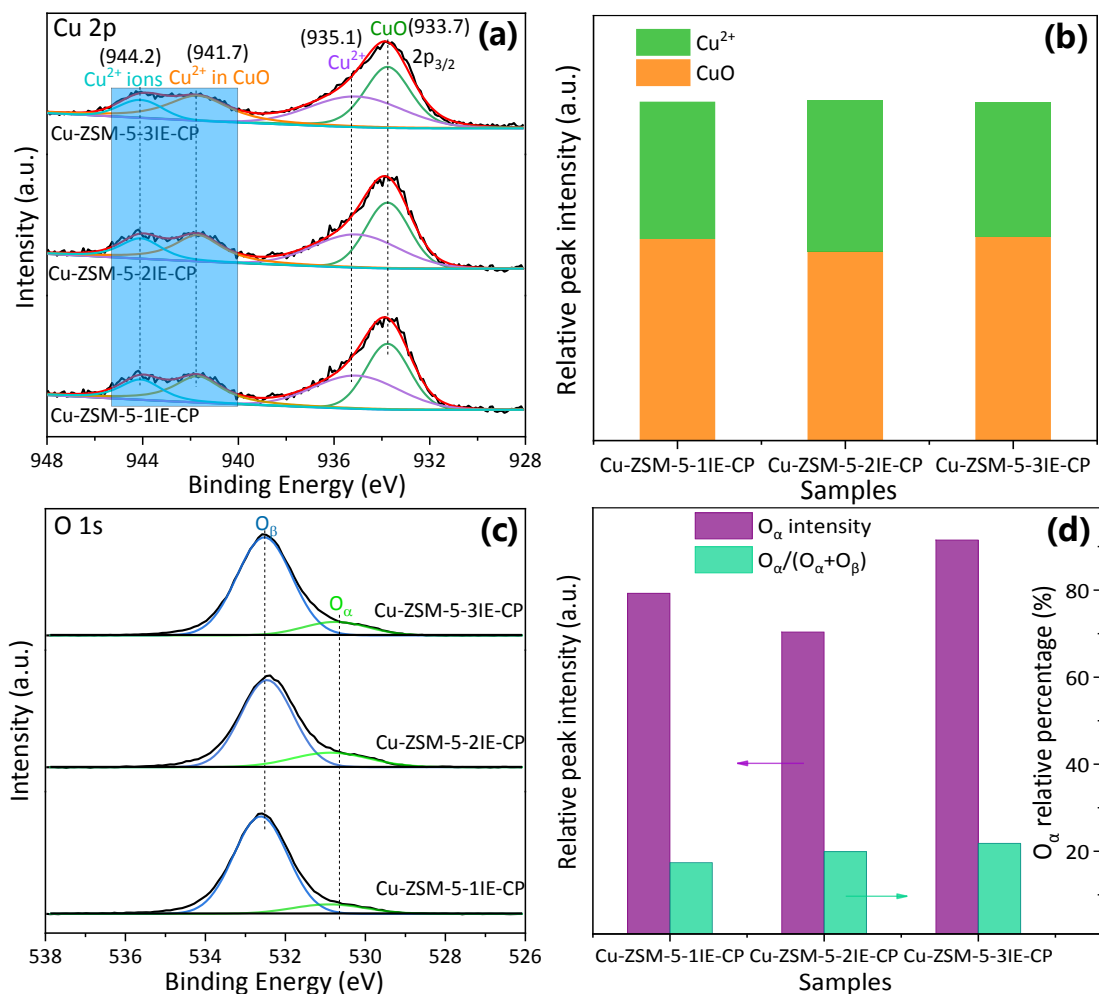


Fig. S11. (a) and (c) XPS spectra of Cu 2p and O 1s for Cu-ZSM-5 catalysts with different ion exchange times. (b) and (d) concentration of different Cu species and O species as a function of ion exchange times semiquantified by the XPS spectra.

Table S3. The surface element concentration of all catalysts in XPS results.

Samples	Cu ²⁺ species		CuO species		oxygen in CuO (O _α)	oxygen in ZSM-5 (O _β)
	Integral area	Percentage (%)	Integral area	Percentage (%)	Integral area	Integral area
Cu-ZSM-5-1IE-CP	3552.17	40.52	5213.86	59.48	5666.31	42975.11
Cu-ZSM-5-2IE-CP	3723.04	44.54	4636.82	55.46	7080.04	30753.39

Cu-ZSM-5	3483.29	39.81	5268.46	60.19	9237.86	57225.81
-3IE-CP						

S11. DFT calculations

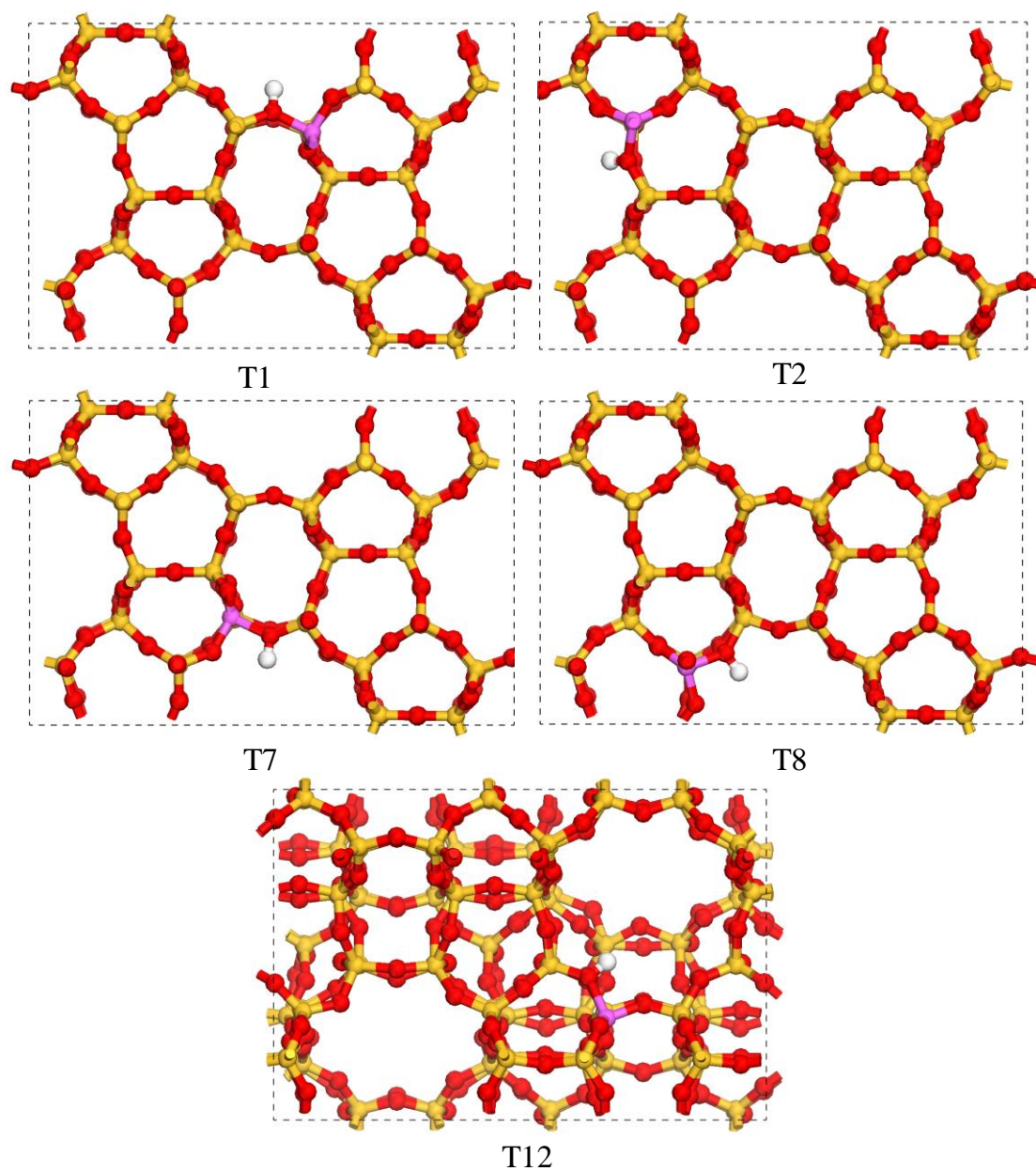


Fig. S12. The optimized structure of different T sites in 10MR in H-ZSM-5 zeolite.

Table S4. Electric energy (E) of different T sites of **optimized** structure in H-ZSM-5 zeolite.

ZSM-5 different T sites	Electric energy/eV
T1	-2270.2461
T2	-2270.1578
T7	-2270.0827
T8	-2270.0321
T12	-2272.1360

The Cu ions (Cu^+ , $\text{Cu}^{2+}\text{-OH}$, $\text{Cu}^{2+}\text{-O}$) located in 10-membered ring could have different position, corresponding to different Si atom sites can be Al to substituted by Al atom. According to the literature, several T sites are selected for the placement of Al atoms, thus we choose T1, T2, T7, T8 and T12 sites in 10MR of H-ZSM-5 to investigate their stability. The electronic energy and optimized structure of different T sites are shown in Table S4 and Fig. S12. One can see from Table S4 that the T12 site have the lowest electronic energy when Al atom substitute Si atom, which indicated that the T12 site is the most stable position. Therefore, T12 site was selected for the following studies.

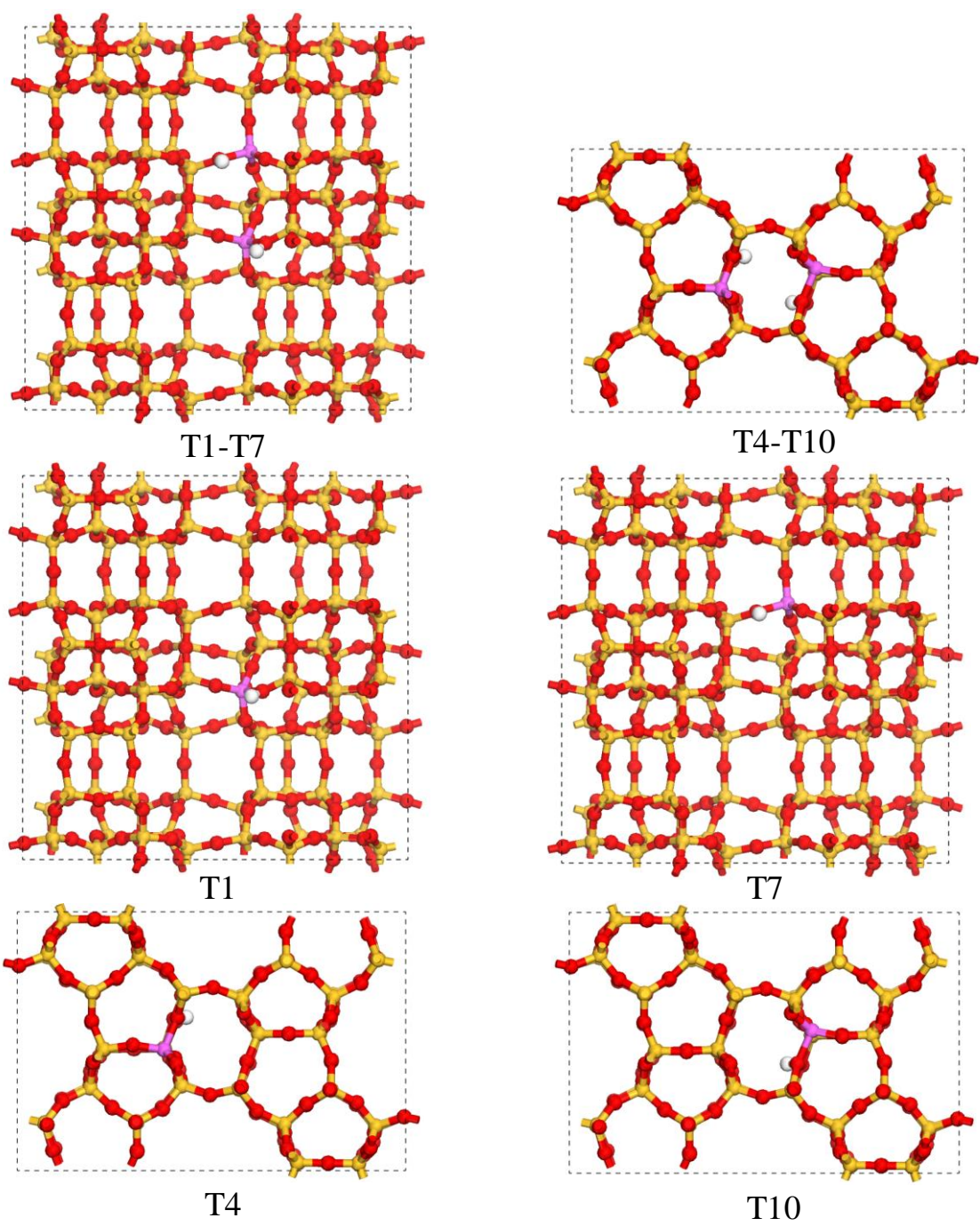


Fig. S13. The optimized structure of different T sites in H-ZSM-5 zeolite.

Table S5. Electric energy (E) of different T sites of α 6MR with 1Al or 2Al in ZSM-5 zeolite.

ZSM-5 different T sites	Electric energy/eV
T1	-2270.1811
T2	-2269.4626
T5	-2269.8320
T7	-2270.0827
T8	-2269.6248
T11	-2269.4214
T1-T7	-2271.1211
T2-T11	-2271.0611
T5-T8	-2269.8746

Table S6. Electric energy (E) of different T sites of β 6MR with 1Al or 2Al in ZSM-5 zeolite.

ZSM-5 different T sites	Electric energy/eV
T1	-2270.0129
T4	-2269.9124
T5	-2269.9254
T7	-2270.0827
T10	-2270.0896
T11	-2269.8668
T1-T7	-2271.0429
T5-T11	-2271.1565
T4-T10	-2271.1850

From the Table S5-6 we can know that one Al located at T1 sites in α 6MR have relative lower energy among the 6 sites, which indicated that T1 is the stable T sites for Al to replace. One Al located at T10 sites in β 6MR have relative lower energy among the 6 sites, which indicated that T10 is the stable T sites for Al to replace. In addition, two Al at T1 and T7 in α 6MR and T4 and T10 in β 6MR possess the lower energy, respectively, which indicates that those are the stable T sites in 6MR. Moreover, the structure with two Al at T4 and T10 possess the lower energy than the two Al at T1 and T7, indicating that the structure with two Al at T4 and T10 is more stable than the structure with two Al at T1 and T7.

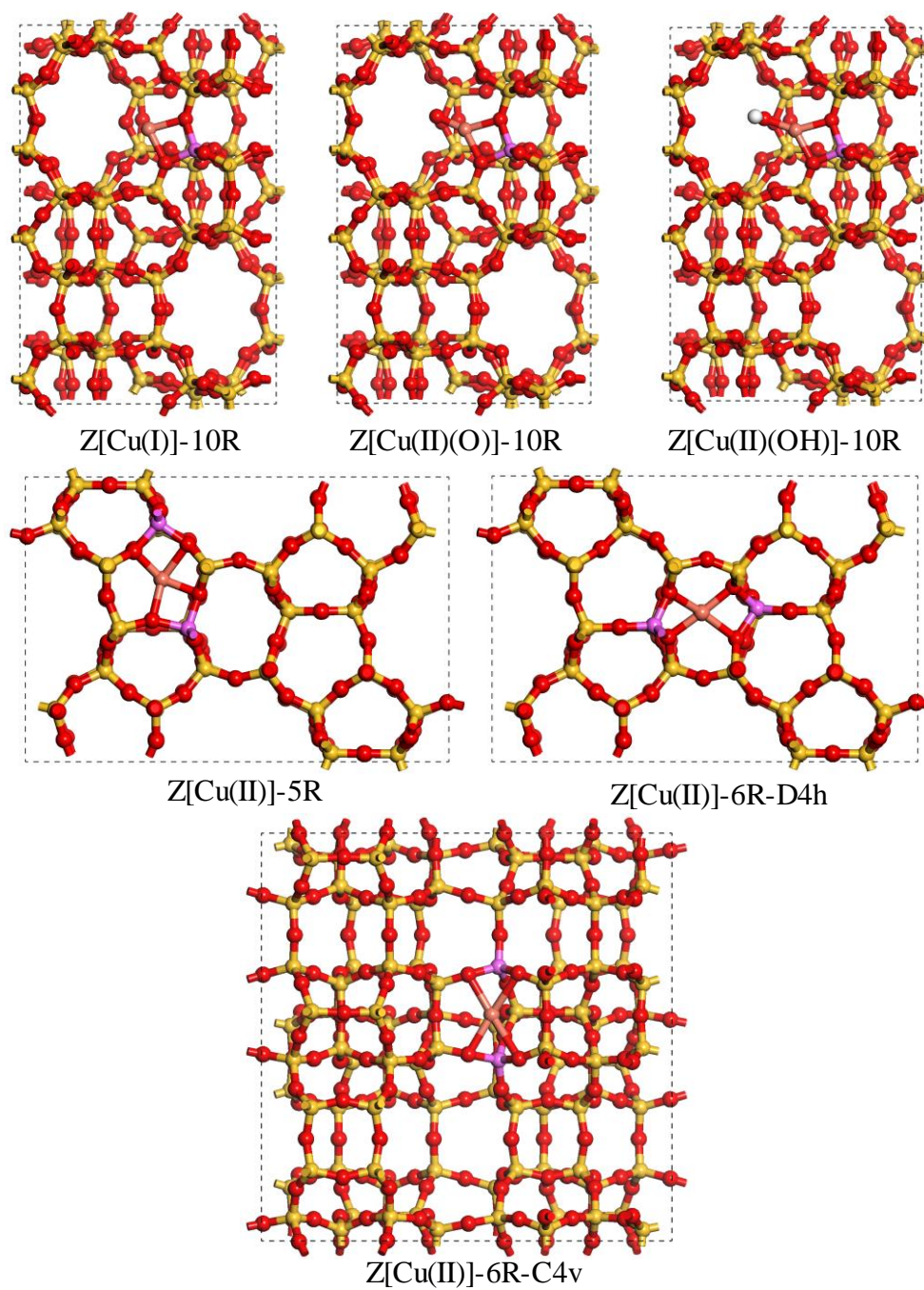
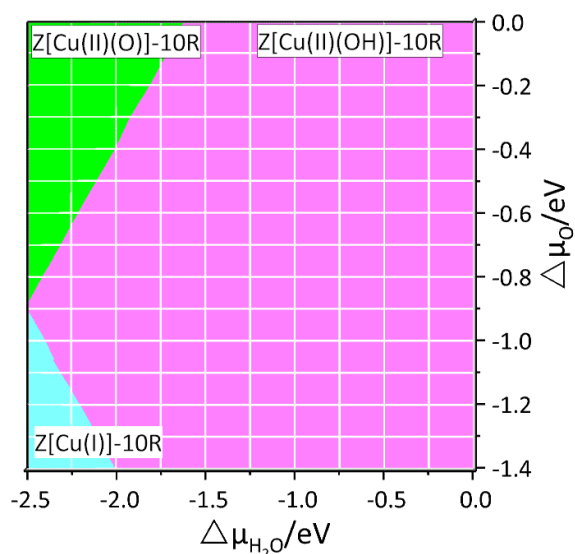


Fig. S14. The optimized structure of different active centers in Cu-ZSM-5 zeolite.

Table S7. Electric energy (E) of different copper active centers structure in ZSM-5 zeolite.

Active centers	Electric energy/eV
Z[Cu(I)]-10R	-2270.7585
Z[Cu(II)(O)]-10R	-2275.8432
Z[Cu(II)(OH)]-10R	-2281.5746
Z[Cu(II)]-5R	-2265.0827
Z[Cu(II)]-6R-D4h	-2266.4093
Z[Cu(II)]-6R-C4v	-2264.4454

The Fig. S14 exhibit the 7 different active centers that very possible formed in Cu-ZSM-5 zeolite. All the structures and optimized relative energy were calculated via DFT and given in the Fig. 14 and Table S7. Those energy were used to calculate the Gibbs free energy (ΔG) of each species showed in main text. The white, red, purple, yellow and green colors are used to distinguish H, O, Al, Si and Cu atoms, respectively.

**Fig. S15.** Phase diagram for Cu species combined with 1Al in Cu-ZSM-5 catalyst as a function of T, P_{H_2O} , and P_{O_2} .

The Fig. S15 showed the stability of Cu species complexes that coordinated with 1Al. This picture illustrated that structure transformation of Cu species with varying T, P_{H_2O} and P_{O_2} , the Z[Cu]-10R, Z[CuO] and Z[CuOH]-10R can be transformed for each other under different reaction conditions. When the H_2O potential decreased, Z[Cu]-10R was the main structure. One can see that the Z[CuOH]-10R have the largest area, indicating that Z[CuOH]-10R may be the most stable Cu species in 1Al structure.

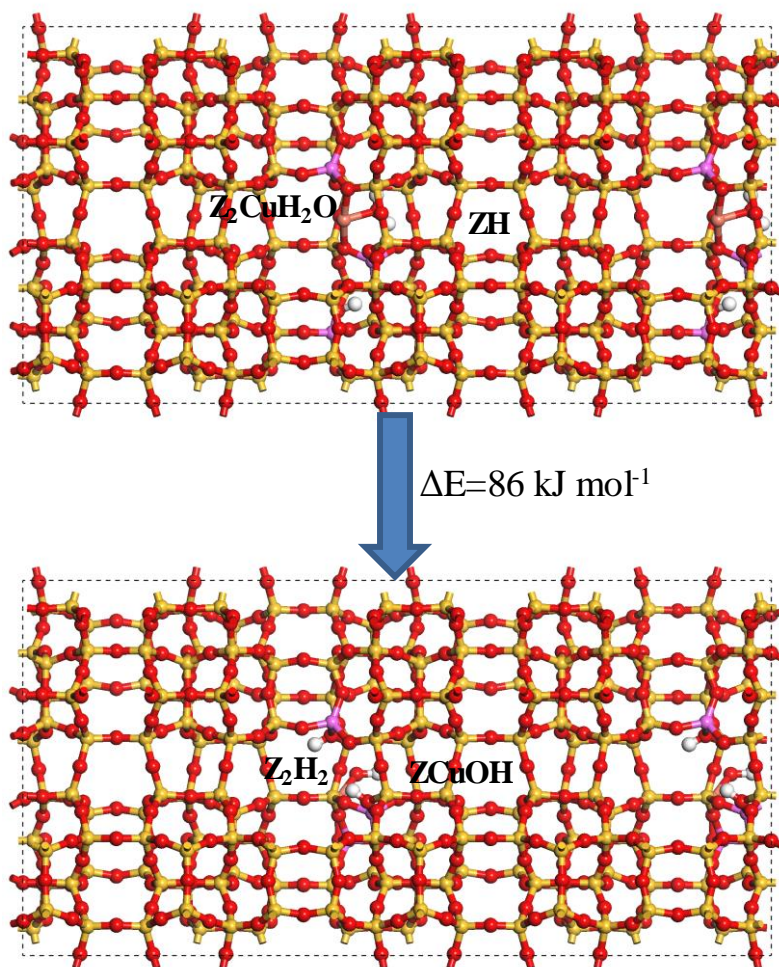


Fig. S16. The exchange energetics of Z_2CuH_2O vs. $ZH/ZCuOH$ in a $1 \times 2 \times 1$ supercell over Cu-ZSM-5 zeolite.

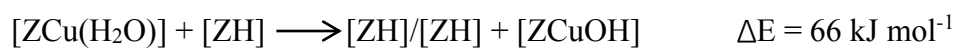


Table S8. Calculated electronic energy of various copper species over 1Al structure in β 6MR.

Copper species	Electronic energy
[ZCu]	-2269.1497
[ZCuO]	-2271.1688
[ZCuO ₂]	-2275.8722
[ZCuOH]	-2277.5832
[ZCu(OH) ₂]	-2287.9668
[ZCuH ₂ O]	-2284.5083
[ZCu-(OH)O ₂]	-2289.4750
[ZCu-OH(H ₂ O)]	-2294.1855
[ZCu-OH(H ₂ O) ₂]	-2307.1407
[ZCu-OH(H ₂ O) ₃]	-2321.7068
[ZCu-OH(H ₂ O) ₄]	-2336.2225
[ZCu-OH(H ₂ O) ₅]	-2351.0315
[ZCu-OH(H ₂ O) ₆]	-2366.0882

Table S9. Calculated electronic energy of various copper species over 2Al structure in β 6MR.

Copper species	Electronic energy
[ZH]/[ZCu]	-2270.0095
[ZH]/[ZCuO]	-2274.0666
[ZH]/[ZCuO ₂]	-2280.4588
[ZH]/[ZCuH ₂ O]	-2285.0527
[Z ₂ CuO ₂]	-2276.4539
[Z ₂ Cu]	-2266.4093
[Z ₂ Cu-H ₂ O]	-2279.402
[Z ₂ Cu-(H ₂ O) ₂]	-2295.034
[Z ₂ Cu-(H ₂ O) ₃]	-2309.5631
[Z ₂ Cu-(H ₂ O) ₄]	-2322.7545
[Z ₂ Cu-(H ₂ O) ₅]	-2338.6605
[Z ₂ Cu-(H ₂ O) ₆]	-2353.3962

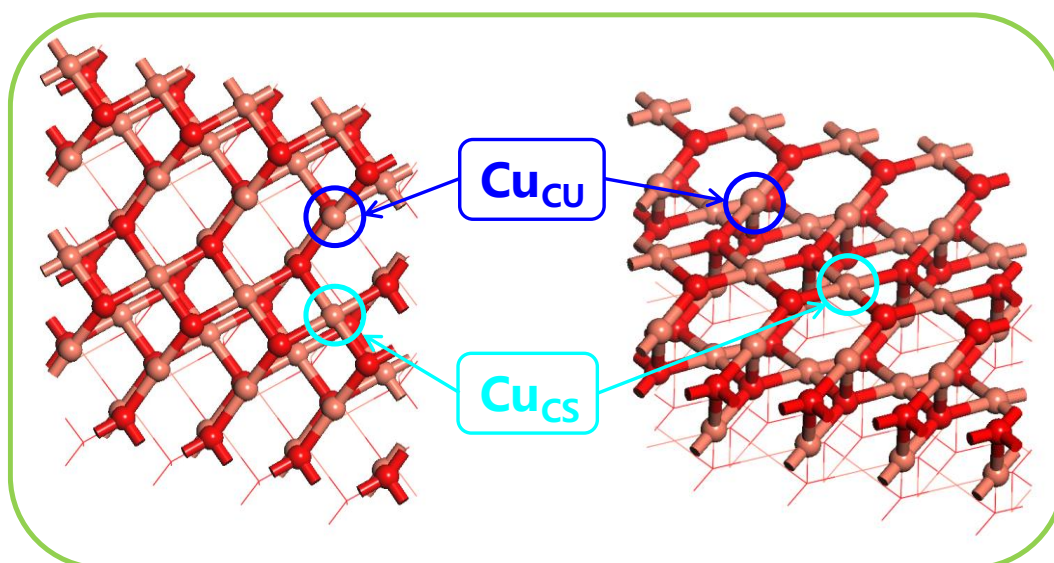


Fig. S17. CuO (111) surface structures after optimization. Left panel show the side view of the supercell, while right panel show the top view of the super cell.

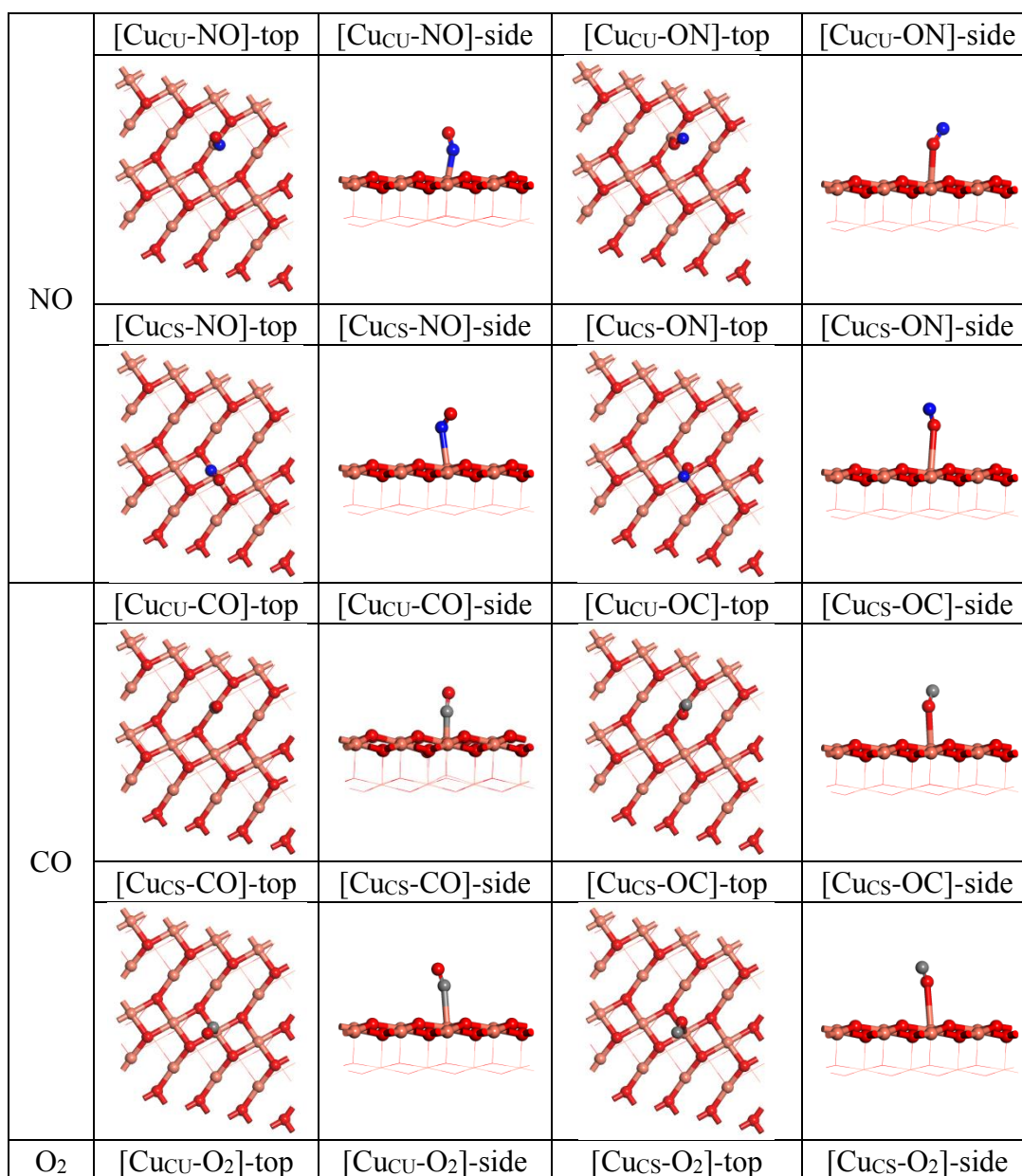
As shown in Fig. S17, two kinds of Cu atoms with different coordination environment existed in CuO (111) surface structure, the Cu atom connected to three O atoms in a state of coordination unsaturation (Cu_{CU}) and another Cu atom connected to four O atoms in coordination saturation (Cu_{CS}). Brown and red balls indicates Cu and O atoms, respectively.

Table S10. Adsorption energies of different reactant molecule on CuO (111) surface structures.

reactant molecule	adsorption species	adsorption energy/eV
CH ₄	Cu _{CU} -CH ₄	-0.26
	Cu _{CS} -CH ₄	-0.25
	Cu _{CU} -CO	-0.59
CO	Cu _{CU} -OC	-0.19
	Cu _{CS} -CO	-0.28
	Cu _{CS} -OC	-0.18
NO	Cu _{CU} -NO	-0.81
	Cu _{CU} -ON	-0.53
	Cu _{CS} -NO	-0.63
O ₂	Cu _{CS} -ON	-0.37
	Cu _{CU} -O ₂	-1.29
	Cu _{CS} -O ₂	-1.28
H ₂	Cu _{CU} -H ₂	-0.12
	Cu _{CS} -H ₂	-0.09

Table S11. Adsorption energies of different reactant molecule on Z[Cu(II)]-6R-D4h of Cu-ZSM-5.

reactant molecule	adsorption species	adsorption energy/eV
NO	Cu-NO	-1.43
ON	Cu-ON	-0.54
CO	Cu-CO	-0.34
OC	Cu-OC	-0.05
O ₂	Cu-O ₂	-1.16
H ₂	Cu-H ₂	-0.08
CH ₄	Cu-CH ₄	-0.03

Table S12. Optimized structure models of different reactant molecule on CuO (111) surface structures.

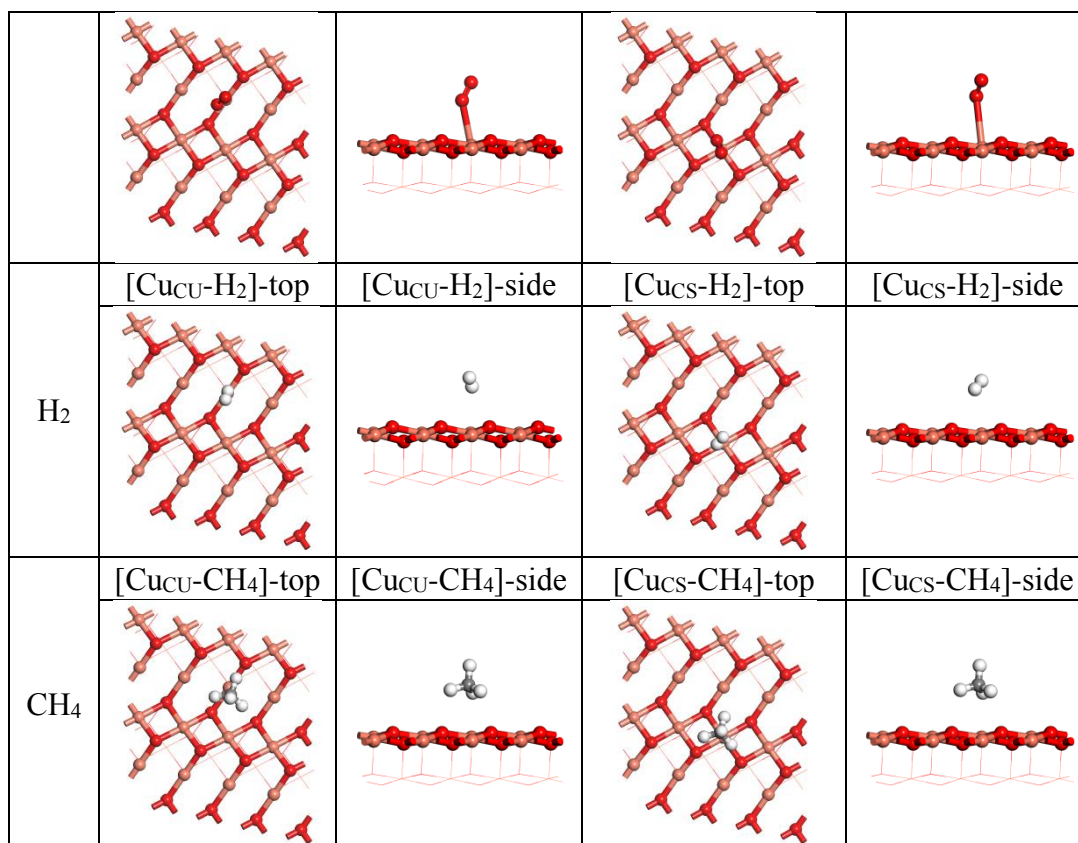
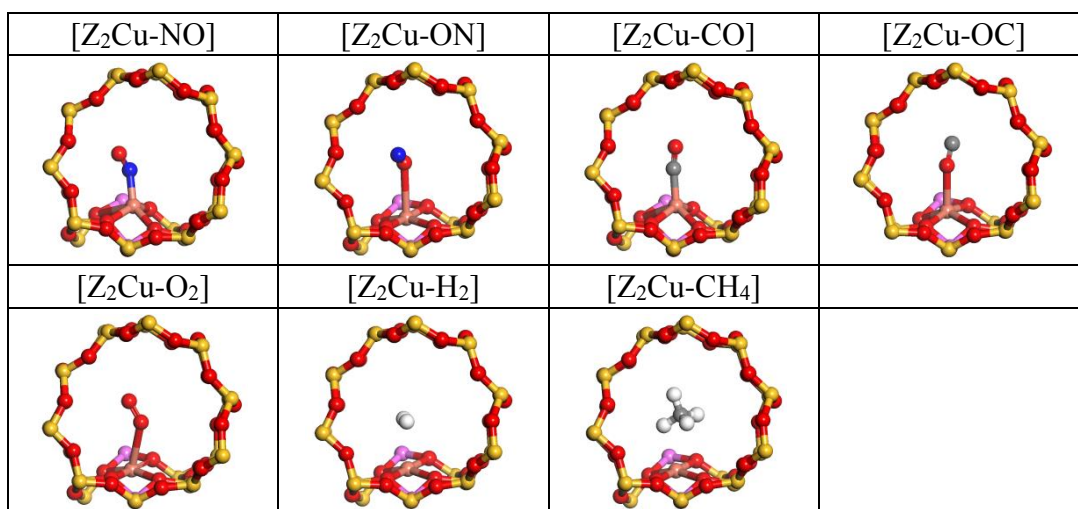


Table S13. Optimized structure models of different reactant molecule on Z[Cu(II)]-6R-D4h of Cu-ZSM-5.



S12. *In situ* DRIFTS studies

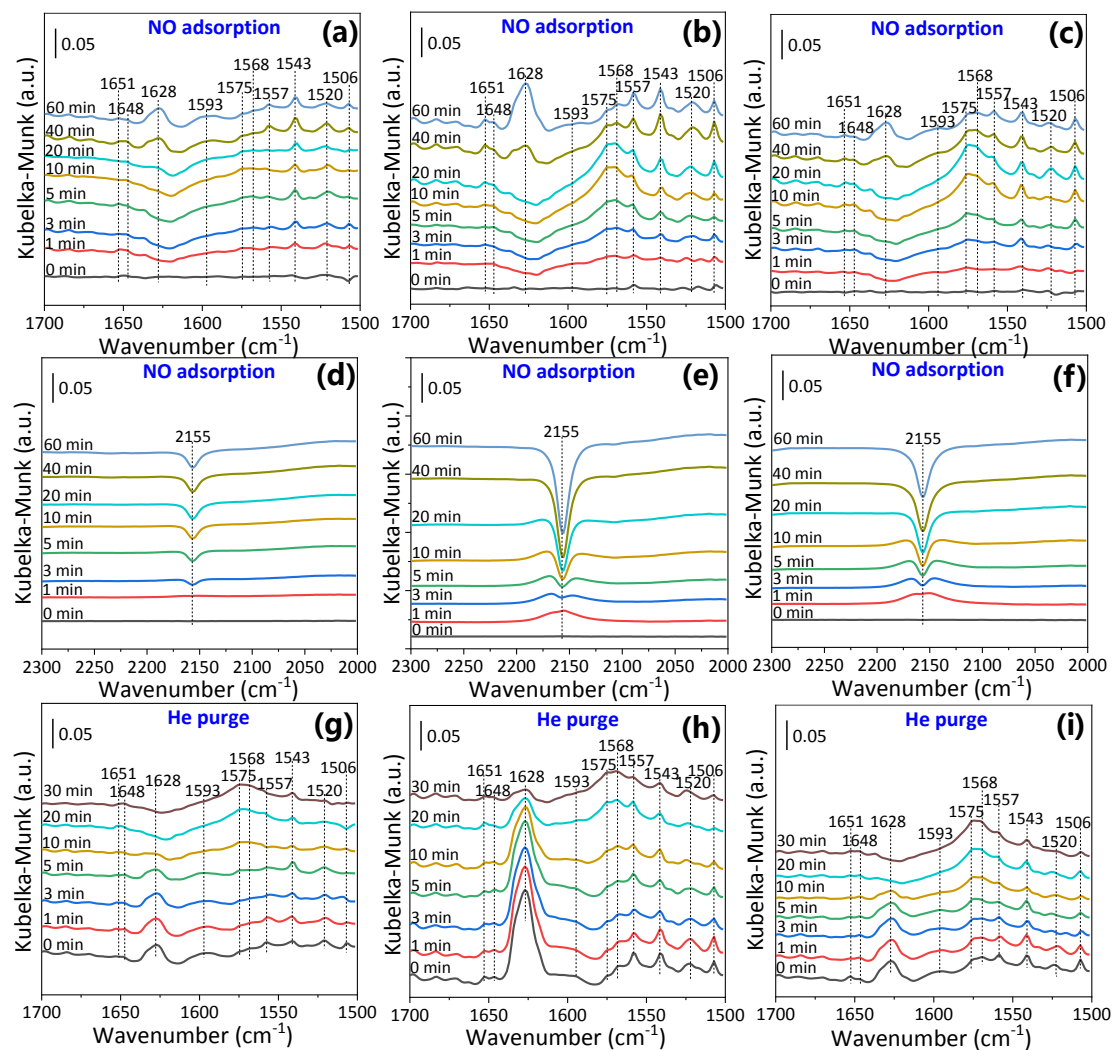


Fig. S18. *In situ* DRIFTS of adsorption of NO + O₂ (a and d, b and e, c and f) and He purging (g, h, and i) over Cu-ZSM-5-IE, Cu-ZSM-5-CP, and Cu-ZSM-5-IE+CP catalysts as the function of reaction time at 280 °C.

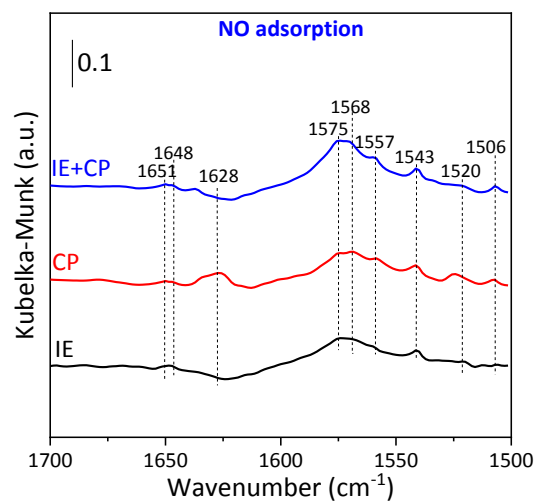


Fig. S19. *In situ* DRIFTS spectra of NO + O₂ over Cu-ZSM-5-IE, Cu-ZSM-5-CP and Cu-ZSM-5-IE+CP catalysts at 280 °C.

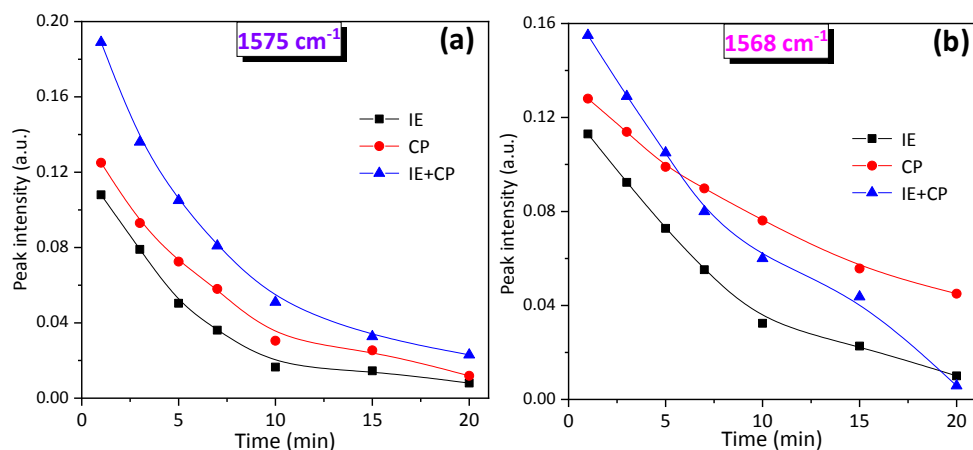


Fig. S20. *In situ* DRIFTS peak intensity of (a) 1575 cm^{-1} and (b) 1568 cm^{-1} on $\text{CO} + \text{H}_2 + \text{CH}_4$ that reacted with preadsorbed $\text{NO} + \text{O}_2$, as function of reaction time at $280\text{ }^\circ\text{C}$.

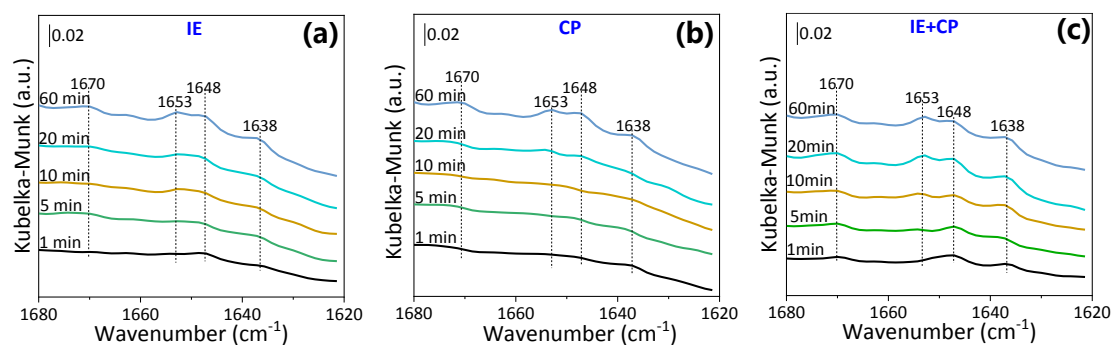


Fig. S21. *In situ* DRIFTS of $\text{CO} + \text{H}_2 + \text{CH}_4$ that reacted with preadsorbed $\text{NO} + \text{O}_2$ on (a) Cu-ZSM-5-IE, (b) Cu-ZSM-5-CP, and (c) Cu-ZSM-5-IE+CP catalysts as the function of reaction time at $280\text{ }^\circ\text{C}$.

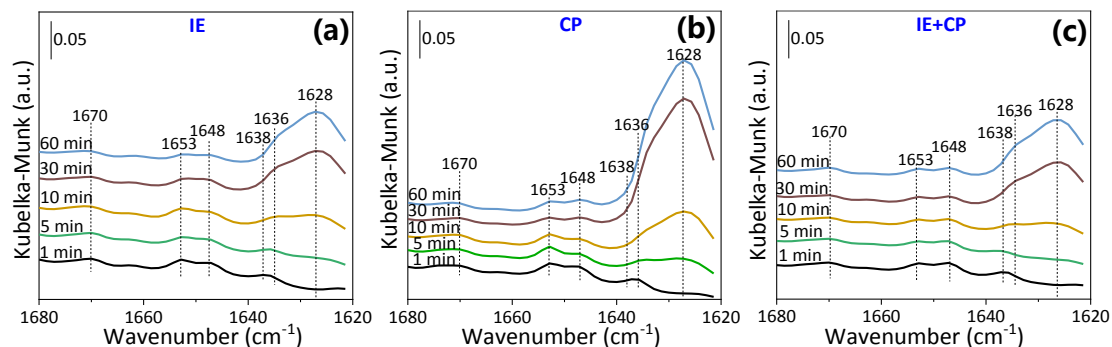


Fig. S22. *In situ* DRIFTS of the reaction between NO + O₂ and adsorbed reductants on (a) Cu-ZSM-5-IE, (b) Cu-ZSM-5-CP, and (c) Cu-ZSM-5-IE+CP catalysts as the function of reaction time at 280 °C.

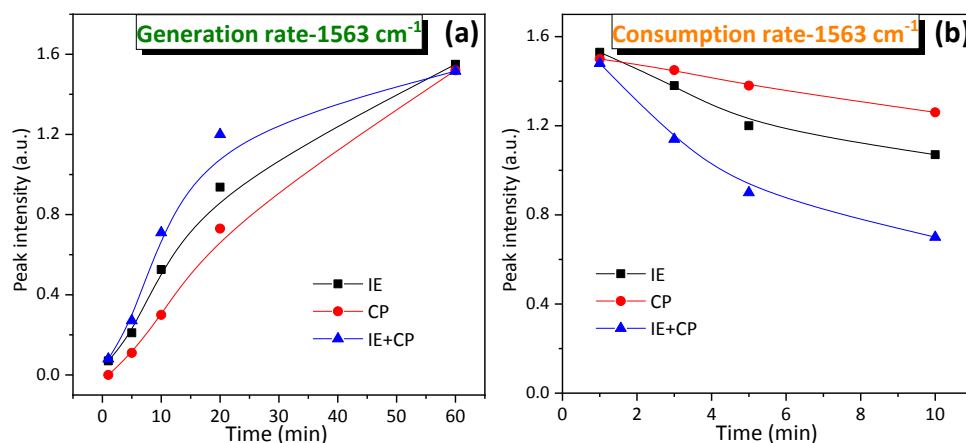


Fig. S23. (a) The generation rates of 1563 cm⁻¹ on CO + H₂ + CH₄ that reacted with preadsorbed NO + O₂ and (b) the consumption rates of 1563 cm⁻¹ on the reaction between NO + O₂ and adsorbed reductants as function of reaction time at 280 °C.

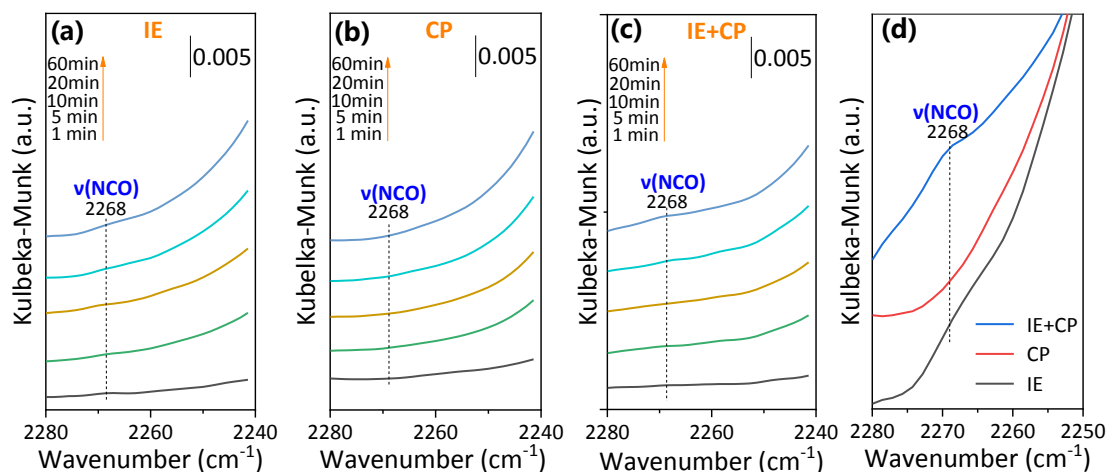


Fig. S24. *In situ* DRIFTS of CO + H₂ + CH₄ that reacted with preadsorbed NO + O₂ on (a) Cu-ZSM-5-IE, (b) Cu-ZSM-5-CP, and (c) Cu-ZSM-5-IE+CP catalysts as the function of reaction time and (d) the spectra of three samples after the reaction for 60 min at 250 °C.

References

1. B. Chen, R. Xu, R. Zhang and N. Liu, Economical way to synthesize SSZ-13 with abundant ion-exchanged Cu⁺ for an extraordinary performance in selective catalytic reduction (SCR) of NO_x by ammonia, *Environ. Sci. Technol.* **2014**, 48, 13909-13916.
2. C.J.G. Vandergrift, A.F.H. Wielers, B.P.J. Joghi, J. Vanbeijnum, M. Deboer, M. Versluijshelder and J.W. Geus, Effect of the Reduction Treatment on the Structure and Reactivity of Silica-Supported Copper Particles, *J. Catal.* **1991**, 131, 178-189.
3. S. Xia, R. Nie, X. Lu, L. Wang, P. Chen and Z. Hou, Hydrogenolysis of glycerol over Cu_{0.4}/Zn_{5.6-x}Mg_xAl₂O_{8.6} catalysts: The role of basicity and hydrogen spillover, *J. Catal.* **2012**, 296, 1-11.
4. G. Kresse and J. Hafner, Ab initio molecular dynamics for open-shell transition metals, *Physical Review B* **1993**, 48, 13115.
5. G. Kresse and D. Joubert, From ultrasoft pseudopotentials to the projector augmented-wave method, *Physical review B* **1999**, 59, 1758.
6. J.P. Perdew, K. Burke and M. Ernzerhof, Generalized gradient approximation made simple, *Phys. Rev. Lett.* **1996**, 77, 3865.
7. Database of Zeolite Structures, <http://www.iza-structure.org/databases/>.
8. D. Stull and Prophet, JANAF Thermochemical Tables, National Bureau of Standards, NSRDS-NBS 1971.
9. C. Paolucci, A.A. Verma, S.A. Bates, V.F. Kispersky, J.T. Miller, R. Gounder, W.N. Delgass, F.H. Ribeiro and W.F. Schneider, Isolation of the copper redox steps in the standard selective catalytic reduction on Cu-SSZ-13, *Angew. Chem.*

Int. Ed. Engl. **2014**, 53, 11828-11833.